



Calibration and Validation of a FAST Floating Wind Turbine Model of the DeepCwind Scaled Tension-Leg Platform

Preprint

G. Stewart and M. Lackner
University of Massachusetts

A. Robertson and J. Jonkman
National Renewable Energy Laboratory

A. Goupee
University of Maine

*To be presented at the 22nd International Offshore and Polar Engineering Conference
Rhodes, Greece
June 17-22, 2012*

NREL is a national laboratory of the U.S. Department of Energy, Office of Energy Efficiency & Renewable Energy, operated by the Alliance for Sustainable Energy, LLC.

Conference Paper
NREL/CP-5000-54822
May 2012

Contract No. DE-AC36-08GO28308

NOTICE

The submitted manuscript has been offered by an employee of the Alliance for Sustainable Energy, LLC (Alliance), a contractor of the US Government under Contract No. DE-AC36-08GO28308. Accordingly, the US Government and Alliance retain a nonexclusive royalty-free license to publish or reproduce the published form of this contribution, or allow others to do so, for US Government purposes.

This report was prepared as an account of work sponsored by an agency of the United States government. Neither the United States government nor any agency thereof, nor any of their employees, makes any warranty, express or implied, or assumes any legal liability or responsibility for the accuracy, completeness, or usefulness of any information, apparatus, product, or process disclosed, or represents that its use would not infringe privately owned rights. Reference herein to any specific commercial product, process, or service by trade name, trademark, manufacturer, or otherwise does not necessarily constitute or imply its endorsement, recommendation, or favoring by the United States government or any agency thereof. The views and opinions of authors expressed herein do not necessarily state or reflect those of the United States government or any agency thereof.

Available electronically at <http://www.osti.gov/bridge>

Available for a processing fee to U.S. Department of Energy and its contractors, in paper, from:

U.S. Department of Energy
Office of Scientific and Technical Information
P.O. Box 62
Oak Ridge, TN 37831-0062
phone: 865.576.8401
fax: 865.576.5728
email: <mailto:reports@adonis.osti.gov>

Available for sale to the public, in paper, from:

U.S. Department of Commerce
National Technical Information Service
5285 Port Royal Road
Springfield, VA 22161
phone: 800.553.6847
fax: 703.605.6900
email: orders@ntis.fedworld.gov
online ordering: <http://www.ntis.gov/help/ordermethods.aspx>

Cover Photos: (left to right) PIX 16416, PIX 17423, PIX 16560, PIX 17613, PIX 17436, PIX 17721



Printed on paper containing at least 50% wastepaper, including 10% post consumer waste.

Calibration and Validation of a FAST Floating Wind Turbine Model of the DeepCwind Scaled Tension-Leg Platform

Gordon M. Stewart and Matthew A. Lackner
Mechanical Engineering Department, University of Massachusetts
Amherst, Massachusetts, United States

Amy Robertson and Jason Jonkman
National Renewable Energy Laboratory
Boulder, Colorado, United States

Andrew J. Goupee
Mechanical Engineering Department, University of Maine
Orono, Maine, United States

ABSTRACT

To capture energy from high wind resources located offshore in deep water, wind turbines mounted on floating platforms become more economical than fixed-bottom turbines. Accurate modeling of floating wind turbines, which will see increased tower, drivetrain, and blade loading from waves and platform movement, is important for the design process, but there have been few tests conducted with which to compare simulations. With the intent of improving simulation tools, a 1/50th-scale floating wind turbine atop a tension-leg platform (TLP) was designed based on Froude scaling by the University of Maine under the DeepCwind Consortium. This platform was extensively tested in a wave basin at the Maritime Research Institute Netherlands (MARIN) to provide data to calibrate and validate a full-scale simulation model. The data gathered include measurements from static load tests and free-decay tests, as well as a suite of tests with wind and wave forcing. The FAST simulation software developed by the National Renewable Energy Laboratory (NREL) was used, and a full-scale FAST model of the turbine-TLP system was created for comparison to the results of the tests. All comparisons were made at full scale.

Analysis was conducted to validate FAST for modeling the dynamics of this floating system through comparison of FAST simulation results to wave tank measurements. First, a full-scale FAST model of the as-tested scaled configuration of the system was constructed, and this model was then calibrated through comparison to the static load, free-decay, regular wave only, and wind-only tests. Part of the calibration process included modifying the airfoil properties of the wind turbine blades to more accurately characterize the aerodynamic performance achieved in the tests. The FAST model was also modified to better represent the structural response data by introducing additional platform damping and stiffness terms. Next, the calibrated FAST model was compared to the combined wind and wave tests to validate the

coupled hydrodynamic and aerodynamic predictive performance. Limitations of both FAST and the data gathered from the tests are discussed in this paper.

KEY WORDS: Floating offshore wind turbine, tension-leg platform, aero-hydro-servo-elastic modeling, tank testing, model calibration, model validation

INTRODUCTION

Offshore wind has the potential to become a large contributor to the United States' energy portfolio in the future. This is due to the higher quality offshore wind resource as well as the proximity of coastal population centers (Musial et al., 2006). Floating wind turbines have the potential to be placed anywhere in the ocean, from 50-meter (m) water depth or beyond. This is a great benefit, because floating platforms allow offshore wind penetration into places where it may be prohibitive for fixed-bottom offshore turbines. Many of the floating platform designs are able to be towed by boats to be moved relatively easily. This may reduce costs associated with deployment and maintenance.

Floating wind turbines show promise for use in deep water areas, but exhibit increased loading due to inertial effects from floating platform motions. Simulation tools such as FAST (Jonkman and Buhl, 2005) have the capability to model floating platforms; however, there are few sources of experimental data from floating wind platforms with which to validate the models.

With this limitation in mind, the University of Maine (UMaine) has conducted a series of scaled experiments of floating wind turbine platforms as part of the DeepCwind Consortium. These experiments were conducted in MARIN's wave basin in the Netherlands, and included free-decay tests, as well as full wind and wave tests, for three

platform designs (Goupee et al., 2012). This paper will focus on the analysis of the UMaine-designed TLP, but tests were also performed on a semi-submersible platform and a spar buoy. This TLP design was inspired by the Glosten Associates' design (Moon and Nordstrom, 2010).

The simulation tool used in this research to create the model of the TLP experiment was FAST. FAST is a coupled aero-hydro-servo-elastic code that simulates the dynamics of wind turbines in the time domain (Jonkman, 2007). It uses Blade-Element/Momentum theory (BEM) or Generalized Dynamic Wake (GDW) theory with static or dynamic stall to calculate aerodynamic loads, a combined nonlinear multibody dynamics and modal superposition formulation for structural components, a quasi-static mooring line model based on continuous cable theory with stretching, turbine control algorithms, and a hydrodynamic module that calculates wave loading on the platform based on linear radiation and diffraction as well as nonlinear viscous drag for offshore applications.

Floating platforms lose the stiffness associated with the fixed-ground foundations, and gain new degrees of freedom (DOF). The naming convention for the floating platforms' DOF used in this paper can be seen in Fig. 1.

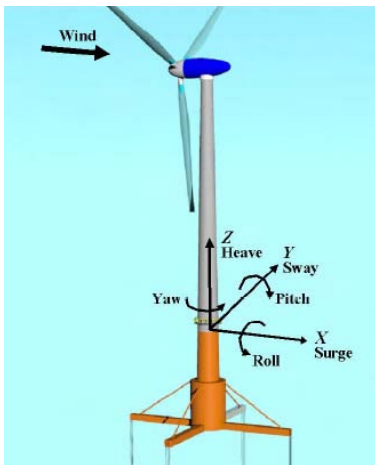


Fig. 1. DOF terminology (Jonkman 2007)

The wind turbine used in the MARIN tests was modeled after the NREL 5-megawatt (MW) reference turbine (Jonkman et al., 2009). Froude scaling is used both to provide the geometry and other properties of the 1/50th-scale experiment as well as the scaling of the output data from the tests. All of the analysis in this paper was done using data and modeling at full scale. For the test data, this means that it must be scaled up to full scale before comparisons are made. Fig. 2 shows a diagram of the TLP used in the experiments,

including sensor locations. Table 1 describes the full-scale physical dimensions of the TLP. The experimental apparatus includes accelerometers in the nacelle and three locations along the tower. There is also an optical displacement sensor located near the tower base, labeled "Motions" in Fig. 2. Load cells are installed between the tower and the platform, between the tower and the nacelle, and on the mooring line fairleads to provide mooring line tension data.

Table 1. Physical Properties of the TLP

TLP Dimensions	
Mass with Turbine (metric ton (mt))	1,361
Displacement (mt)	2,840
Draft (m)	30.0
Center of Mass above Keel (m)	64.1
Mooring Spread Diameter (m)	60.0
Roll Radius of Gyration (m)	52.6
Pitch Radius of Gyration (m)	52.7

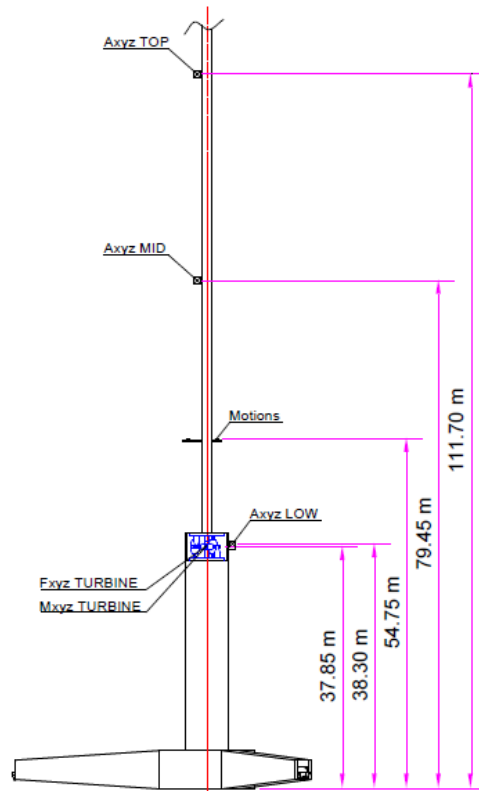


Fig. 2. Sensor location on experimental TLP

The goal of this research was to create, calibrate, and validate a full-scale FAST model of this TLP. The calibration step involved tuning the platform, tower, and aerodynamic parameters in the simulation of the wind turbine to match the data produced by the static equilibrium, decay, regular wave tests, and tests with only aerodynamic loading. The calibrated model was then used to compare to the combined wind and wave tests in an effort to validate FAST as a modeling tool for floating wind turbines.

MODEL CALIBRATION

Wind Turbine Geometry and Mass Properties

The horizontal-axis wind turbine chosen for scale-model construction is the fictitious, albeit extensively studied, NREL 5-MW reference wind turbine (Jonkman et al., 2009). The wind turbine possesses a 126-m rotor diameter and a hub height of 90 m above the still water line (SWL). The flexible tower, which begins 10 m above the SWL, is designed to emulate the mass and stiffness of the OC3-Hywind tower (Jonkman, 2010). The scale-model wind turbine deviates from the standard NREL 5-MW reference wind turbine in a few notable areas. For the model wind turbine, the shaft tilt is 0°, the blade precone is 0°, and the blades are essentially rigid, which is a reasonable approximation of the actual model. The total mass of the rotor inclusive of the hub and three blades is a full-scale equivalent of 122,220 kilograms (kg). All values reported in this paper are full-scale-equivalent values. The nacelle mass is 274,940 kg.

For the physical model, instrumentation cables used for recording all of the wind turbine response data, as well as nacelle accelerations and

tower-top forces, were affixed to approximately the upper two-thirds of the model tower before being looped away to run to the data acquisition system. In FAST, this instrumentation cable is not modeled directly. Instead, the apparent additional weight the platform had to support due to the cables was smeared evenly over the length of the tower for numerical modeling. The distributed stiffness of the tower was assumed to be unaltered by the presence of the cables. Therefore, the distributed bending stiffness for the tower employed for the numerical model was taken directly from the product of the tower material Young's modulus and distributed area moment of inertia. The tower area moment of inertia did not vary smoothly along the length of the tower, with the lower 11.3 m of the tower having a larger outer diameter than the remainder of the tower. The total tower mass, including the additional cable mass, was 302,240 kg. The sensor cable accounts for 137,650 kg of this tower mass. The total topside mass, which included the wind turbine and tower, was 699,400 kg. This value is 16.6% larger than the standard specifications for the combined NREL 5-MW reference turbine and OC3-Hywind tower.

Blade Aerodynamic Properties

Due to the low Reynolds numbers experienced during Froude-scale wind/wave basin testing, the aerodynamic performance of the wind turbine blade airfoil sections (which were geometrically scaled) was significantly altered. To generate the airfoil data required for numerical modeling calibration and validation studies, analyses of the airfoil sections were performed at the low Reynolds numbers for small positive angles of attack using the high-order viscous airfoil analysis panel code XFOil (Drela 1989). However, the analyses were incredibly sensitive to the particular Reynolds number and laminar-to-turbulent transition parameters. Despite the fact that the analysis replicated the general change in performance seen during the testing, the generated lift and drag coefficient curves did not accurately reproduce the model-testing-derived coefficient of thrust and coefficient of performance curves for the wind turbine when utilized in FAST. Therefore, the XFOil curves were used as a guide to create a parameterized set of curves that permitted variations in key lift and drag coefficient parameters, such as lift coefficient stall points and minimum drag coefficients. The parameterized curves were extrapolated for all angles of attack via the Viterna Method (Hansen, 2010). A multi-objective genetic algorithm (e.g. see Deb, 2001) was used to search for the lift and drag coefficient parameters that minimized the error between the FAST predictions and wind-only model test data for the wind turbine coefficient of thrust and coefficient of performance curves simultaneously.

Of the various Pareto-optimal solutions found, the result selected was one which favored a solution that achieved minimal error in the thrust coefficient curve (C_T) while still maintaining some semblance of the measured performance coefficient (C_p). This preference of matching the thrust performance was undertaken because the wind turbine thrust force, and not the rotor torque, is the key driver in the global motions of the floating wind turbine under combined wind and wave loadings. A comparison between the FAST prediction and the test data is shown in Fig. 3.

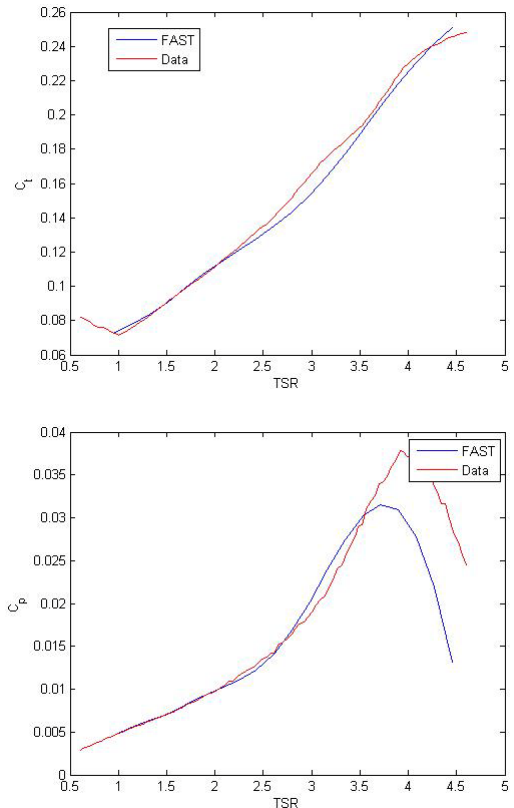


Fig. 3. Comparison of model test data and aerodynamic model for coefficients of thrust and performance versus tip-speed ratio (TSR)

The FAST results in Fig. 3 were generated with no aerodynamic pitching-moment coefficients. As can be seen in Fig. 3, the thrust, and especially the performance coefficients are significantly lower than the NREL 5-MW reference wind turbine. The reason for this, discussed in detail in Martin (2011), is due primarily to laminar separation of the airfoil sections that drastically reduces lift and increases drag. This is especially true for the numerous thick airfoil sections found on the NREL 5-MW blade.



Fig. 4. UMaine TLP model

Initial Model and Static Equilibrium Comparison

Static equilibrium simulations were carried out in FAST with this initial model to check the global characteristics of the model. It was found that, by using the platform volumetric displacement given by MARIN, there was substantial platform heave ringing. When the platform displacement value was reduced by approximately 1% of the original value, the magnitude of this heave ringing was reduced to negligible values. Once this heave motion was eliminated, the tension values in the mooring cables were compared to the experimental values and were found to be in good agreement.

Free-Decay Tests

Free-decay tests were conducted on the experimental TLP by introducing a displacement to a platform DOF and allowing the system to come to rest. Specifically, these tests were conducted to determine the natural frequencies and damping ratios of the various DOFs. Ideally, only one DOF is excited by these tests, but in practice, the tests usually excited more than one DOF. By reviewing the experimental time series, the initial displacements could be extracted and applied to the FAST model.

The data from the optical displacement sensor was found to be inaccurate for the rotational DOFs (pitch, roll, and yaw). This is most likely due to the relatively small displacement of the TLP in these DOFs compared to the rotational sensing accuracy. For this reason, the acceleration data was used instead of the displacement data as a basis for comparison between FAST and the tests.

To tune the natural frequencies and damping ratios of the platform DOFs in FAST, an additional FAST input file was created that gives the user the capability of adding stiffness and damping to each platform DOF. Using this addition, the natural frequencies and damping ratios were iteratively tuned to match the values found in the decay tests. This was done using a frequency-domain analysis of the test data and the FAST output. The stiffness and damping parameters were tuned by hand using a visual comparison of the frequency response of the experiment to the simulation.

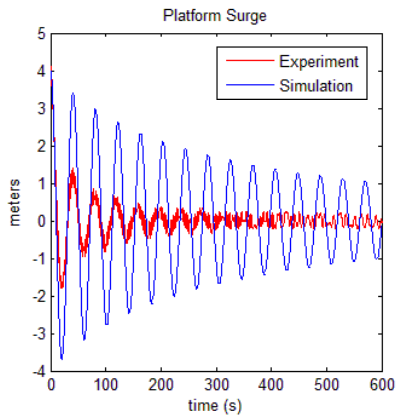


Fig. 5. Un-tuned surge decay test surge displacements

Surge Decay Test. For the surge decay test, the comparison of the surge DOF displacement from the un-tuned FAST model and the test can be seen in Fig. 5. In this test, the platform was displaced the full-scale equivalent of 4 m in the surge direction. Figures 6 and 7 show the acceleration and acceleration power spectral density (PSD) of the surge DOF, respectively.

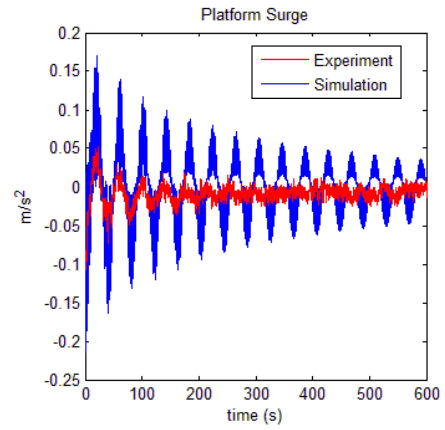


Fig. 6. Un-tuned surge decay acceleration

Figs. 5-7 show that the FAST model is producing a surge frequency that closely matches the test data, but the FAST simulation model is under-damped for this DOF. In addition, it can be seen in Fig. 7 that the heave DOF is highly under-damped in the FAST model as well. This is most likely due to the effect of the sensor cable bundle mentioned earlier, as well as possible under-predictions of damping due to the neglecting of viscous drag in the numerical model. The simulation shows large peaks due to the coupling of the heave, pitch, and tower-bending DOFs with the surge DOF that do not show up in the test. As there is no excitation in the sway, roll, or yaw DOFs, these DOFs can be ignored for this test.

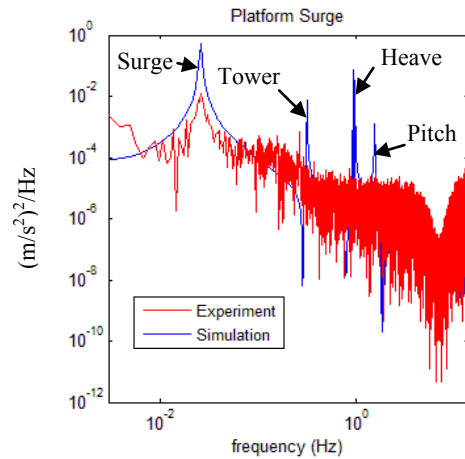


Fig. 7. Un-tuned surge decay acceleration PSD

Fig. 8 shows the PSD of the platform acceleration with additional damping implemented for the surge and heave DOFs. The surge damping has been increased by 1×10^5 Ns/m, increasing the damping ratio from 0.01 in the un-tuned case to approximately 0.094. The heave damping ratio has been changed from near zero in the un-tuned case to 0.57.

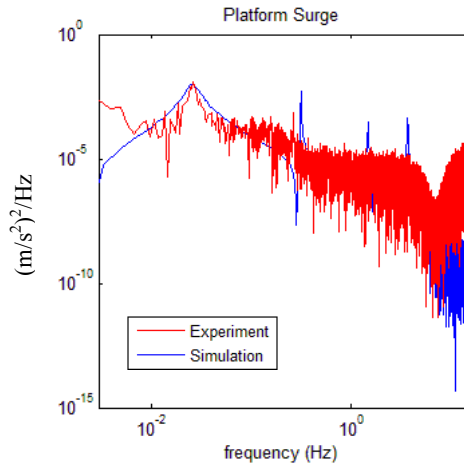


Fig. 8. Tuned surge acceleration PSD

One issue with the tuned model can be seen in Fig. 9. The data from the experiment indicates non-linear, amplitude-dependent damping. In other words, the value of the damping constant for the experiment is larger for larger amplitude motion, and reduces as the motion damps out. This phenomenon could be a result of the sensor cable bundle, or more likely viscous drag, where damping is proportional to velocity squared, and should be investigated in future work. For the scope of this study, the damping is approximated as linear in FAST.

Further Decay Tests. This method of tuning was carried out for the other DOF decay tests. Due to difficulties in determining the exact initial conditions of each test, only approximate constants could be determined from the decay tests. For example, one of the pitch-decay tests was conducted by pushing the top of the tower in the pitch direction. This method of excitation produces a substantial amount of initial tower bending which is hard to quantify from the test data. The other pitch-decay test was conducted by pushing on the leg of the TLP to impart an initial pitch. Because of these inaccuracies with the free-decay tests, the plane-progressive (regular) wave tests were used for further calibration.

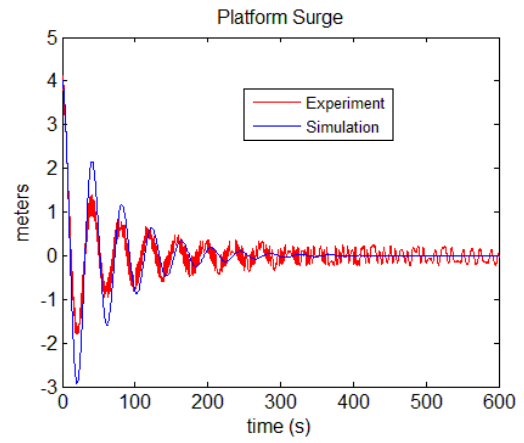


Fig. 9. Tuned surge DOF displacement

Regular Wave Tests

The tests conducted in the wave basin included seven regular wave tests with no wind excitation. These tests used a single-frequency long-crested wave input. FAST has the capability to generate these types of waves, so the inputs for the experiment and model were very similar; resulting in a stronger comparison than the decay tests. Fig. 10 shows the surge displacement for one of the regular wave tests and includes the surge damping tuning from the surge decay test.

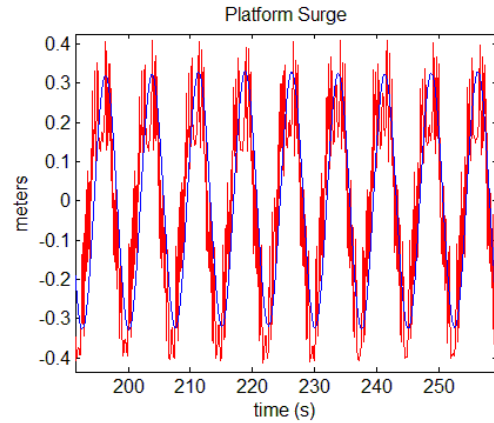


Fig. 10. Surge displacement for regular wave test with Height = 1.92 m, Period = 7.5 s

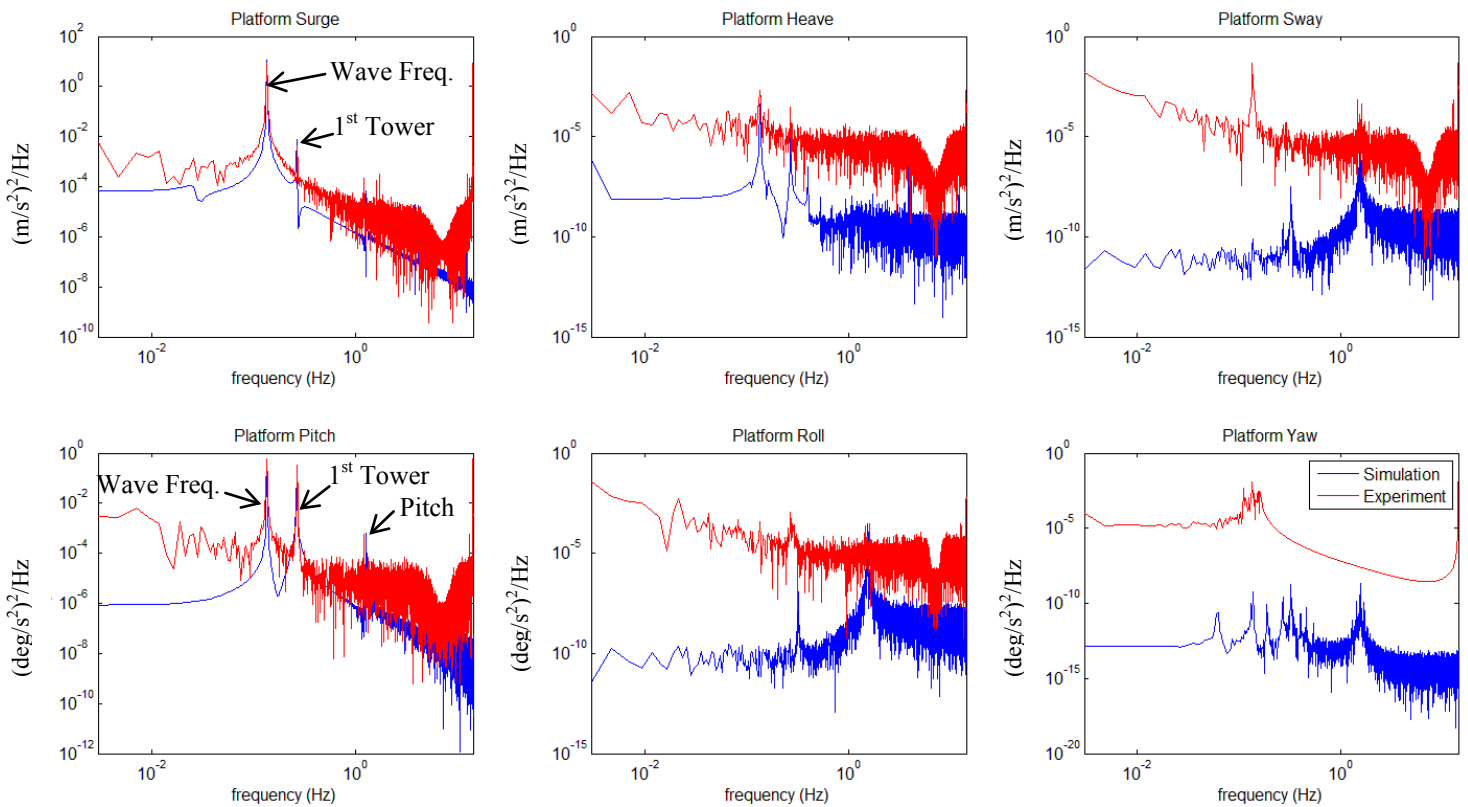


Fig. 11. Acceleration frequency response for regular wave test

Due to the inaccuracies in the free-decay tests, some of the platform parameters were further tuned using the frequency response of one of the regular wave tests. Fig. 11 shows a plot of the acceleration frequency response for all six DOFs, after tuning. In the upper left graph of the platform-surge frequency response, the simulation-surge response at the wave frequency agrees with the experiment well, and the response at the first tower-bending mode agrees as well. In the plot of the pitch-acceleration frequency response (lower left), the wave frequency, the first tower-bending mode, and the pitching frequency are indicated.

Tuning the pitch and tower-bending frequency proved to be a challenge. The mode shapes of the tower were initially determined by the University of Maine using an in-house finite-element method (FEM) code, and as confirmation, an analysis was conducted using BModes, an NREL FEM mode shape software (Bir 2008). The difficulty with this procedure is that the tower-bending mode and the pitch mode are highly coupled. In order to find the proper mode shapes, an iterative process was conducted with BModes by reducing the pitch stiffness from 5.8×10^{10} Newton-meters/radian (Nm/rad) to 2.6×10^{10} Nm/rad until both the pitch and tower-bending frequencies aligned with the tests.

The other four DOFs, heave, sway, roll, and yaw, were excited more by the waves in the experiment than in the simulations. Of note is that the magnitude of these DOFs is much smaller than the surge and pitch magnitudes. These discrepancies are most likely due to experimental imbalances in the mooring lines or in the mass symmetry of the experimental TLP.

Summary of Model Calibration

A summary of the changes to the DOF damping ratios and frequencies can be seen in Table 2. In addition to the changes seen in the table, the

tower mode shapes were changed, which caused the change in tower frequency seen in the table.

Table 2. Summary of Calibration

	Original Nat. Freq. (Hz)	Tuned Nat. Freq. (Hz)	Original Damping Ratio	Tuned Damping Ratio
Surge	0.025	0.025	0.01	0.098
Sway	0.025	0.025	0.01	0.098
Heave	0.96	0.96	5.1×10^{-7}	0.57
Roll	1.52	1.52	0.0050	0.0050
Pitch	1.56	1.27	0.0051	0.0050
Yaw	0.058	0.058	0.047	0.047
First Tower Fore-Aft	0.32	0.26	0.006	0.006
First Tower Side-Side	0.32	0.26	0.006	0.006

MODEL VALIDATION

In this section, the simulations that were run to date for the model validation step are presented. Two experiments with constant wind and operational waves were simulated in FAST. More simulations will be conducted in future work on this project. In these tests, the time series of the wave input was not replicated directly, but the spectrum of the wave input was the same as the experiment. The first experiment that was simulated used a 7-m/s wind speed, and a wave spectrum with a 2-

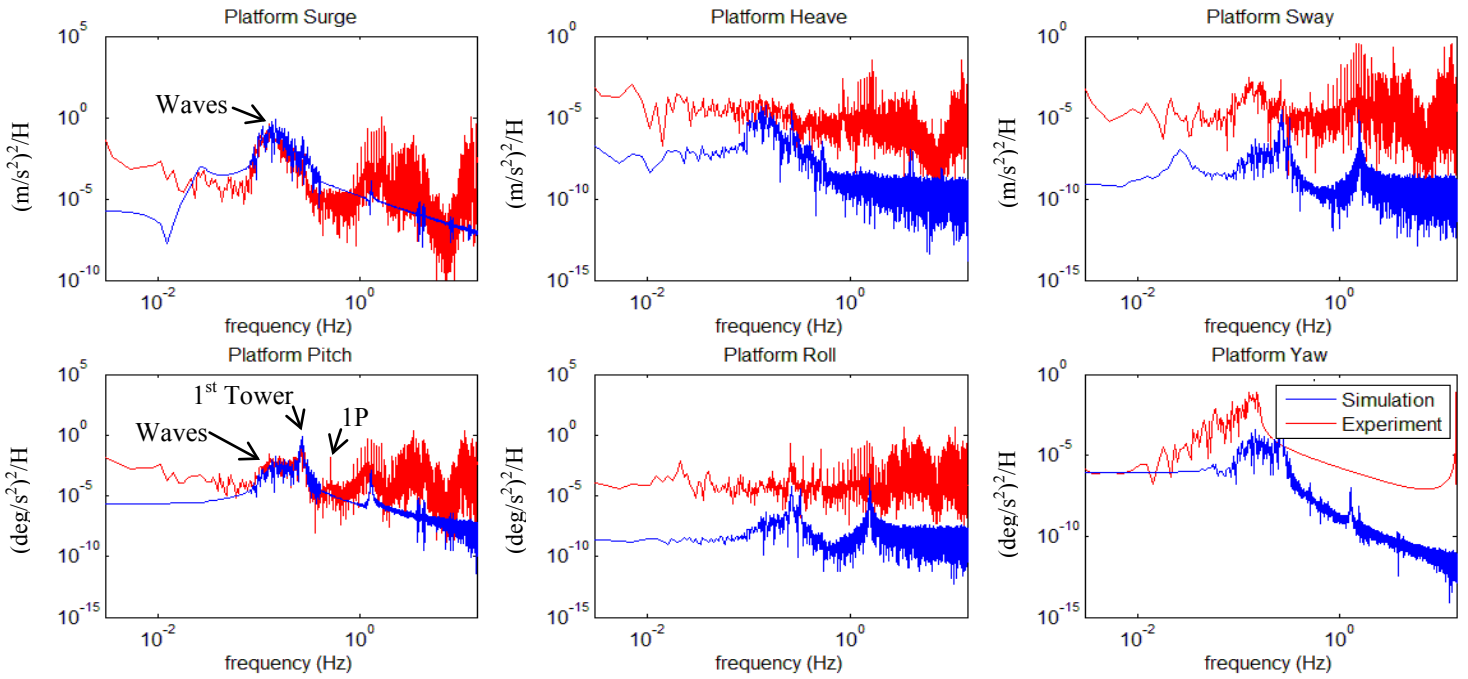


Fig. 12. Acceleration frequency response for low operational wave test and steady 7 m/s wind

m significant height, a 7.5-s peak-spectral period, and a peak shape parameter of 2.0. The pitch of the blades was held at a constant 6.4 degrees, and the rotor was held at a constant speed of 4.95 revolutions per minute (RPM) in both the simulation and the experiment. The values for pitch and rotor speed differed from the normal NREL 5-MW specification as these values were chosen to match simulated rotor thrust with the augmented aerodynamic performance of the 1/50th-scale model.

Fig. 12 shows the frequency response of the acceleration of the DOFs for this first validation case. The discrepancies in the frequency range lower than the wave frequencies were most likely due to fluctuations in the experimental wind speed. Similar to the regular wave response, the lower frequency modes were captured well by the simulation, but the simulation diverged from the experiment for higher frequency modes.

The difference in energy between the experiments and the simulations at these higher frequencies could mean that the FAST model needs higher frequency modes, that the simulation model was improperly calibrated, or that the sensors used in the experiments had errors or noise at these high frequencies. Further research is required to determine what combination of these three options is present.

In the pitch frequency response in Fig. 12, the experiment shows a peak at the rotor frequency (1P). The FAST simulation shows no pitch excitation at this frequency. Causes of 1P excitation are indicative of a rotor imbalance in the experiment, which was not simulated in FAST. Future models may address this issue of rotor imbalance.

The second case that was simulated was an experiment with much higher wind and wave loading. The steady wind speed for this test was

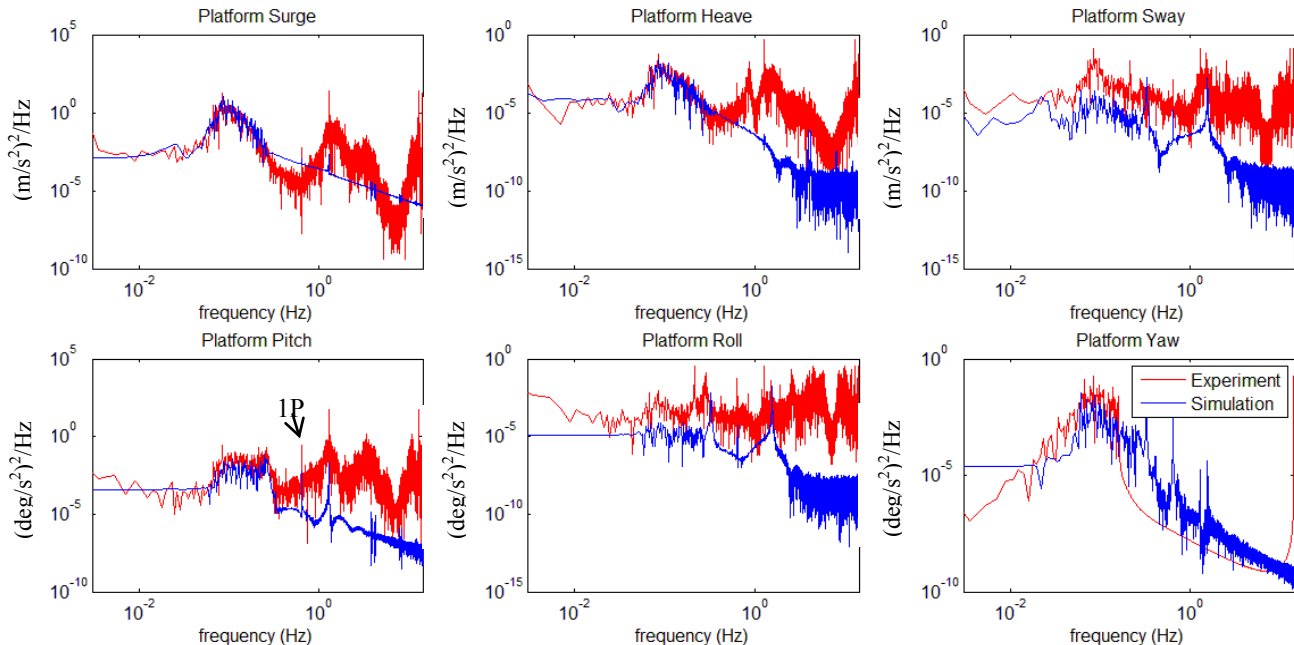


Fig. 13. Acceleration frequency response for high operational wave test and steady 21 m/s wind

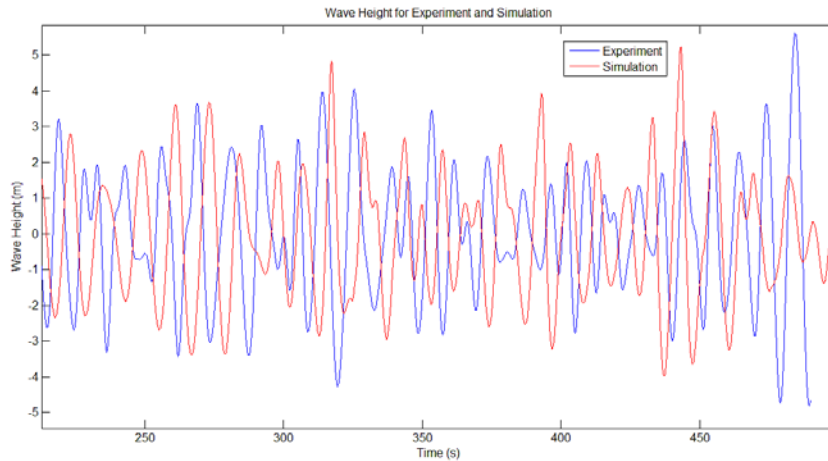


Fig. 14. Wave time series

21 m/s, the wave height was 7.1 m, the peak-spectral period was 12.1 s, and the shape factor was 2.2. Fig. 13 shows the acceleration frequency response in each DOF. Due to the high wind and wave loading, the simulated TLP exhibited an excessive increase in pitch angle magnitude during a large wave event, causing the simulation to end prematurely. Fig. 14 shows a plot of the experimental and simulated wave heights. The simulation crashed after the large wave seen at the end of the time series. Because the blade pitch was constant in all of these tests, the rotor thrust produced by the 21-m/s wind was enough to cause a 12-m surge. These factors combined to cause excessive pitch motion. The amplitude of the pitch motion leads to a slack-line event in FAST, in which the tension in the rear mooring line goes to zero. This phenomenon was seen in the experiment as well, which is an encouraging sign for modeling accuracy.

In Fig. 13, there is reasonable agreement between the response of the experiment and the response of the simulation. This case produced the most consistent results seen to date for the sway, heave, roll, and yaw DOFs and could be caused by a phenomenon similar to the non-linear damping seen in Fig. 9. As the amplitude of motion becomes higher, the damping values of various degrees of freedom may increase in the experiment, which is closer to what the simulation is showing.

With the higher wind speed of this experiment, the 1P excitation is showing up in the FAST simulation, as indicated in the pitch response in Fig. 13. The cause of this 1P excitation is being investigated.

CONCLUSIONS

This paper presents a calibrated FAST model built to represent a scaled model of a floating wind turbine mounted on a TLP. A preliminary validation study of this model was also conducted. After calibrating the FAST model, the comparison between the simulations and experiment was very good in the wave-excitation frequency range in the DOFs that were directly forced by the wind and waves. Discrepancies between the simulations and experiment were seen in other areas, however. As a result, more research is needed in order to determine if the differences between the model and experiment are due to errors in model calibration, sensor error, test errors, or true underperformance of the simulation tool. Work is ongoing in this area.

ACKNOWLEDGEMENTS

The financial support for obtaining the DeepCwind test data from the U.S. Department of Energy through DeepCwind Grants DE-

EE0002981 and DE-EE0003728, the National Science Foundation through Grant IIP-0917974, and the University of Maine is gratefully acknowledged by the authors.

REFERENCES

- Bir, G (2008). *NWTC Design Codes (BModes by Gunjit Bir)*. <http://wind.nrel.gov/designcodes/preprocessors/bmodes/>, Last modified March 20, 2008, Accessed March 20, 2008.
- Deb, K (2001). *Multi-Objective Optimization Using Evolutionary Algorithms*. John Wiley & Sons, LTD, Chichester.
- Drela, M (1989). "XFOIL: An Analysis and Design System for Low Reynolds Airfoils," *Conference on Low Reynolds Airfoil Aerodynamics, University of Notre Dame*.
- Goupee, AJ, Koo, BJ, Lambrakos, KF, and Kimball, RW (2012). "Model Tests for Three Floating Wind Turbine Concepts," *Offshore Technology Conference*.
- Hansen, C (2010). *NWTC Design Codes (Airfoil Prep)*. <http://wind.nrel.gov/designcodes/preprocessors/airfoilprep/>, Last modified March 9, 2010, Accessed November 2011.
- Jonkman, J, and Buhl, M (2005). "FAST User's Guide", Technical Report, National Renewable Energy Laboratory.
- Jonkman, J (2007). *Dynamics Modeling and Loads Analysis of an Offshore Floating Wind Turbine*. PhD Dissertation.
- Jonkman, J, Butterfield, S, Musial, W, and Scott, G (2009). "Definition of a 5-MW Reference Wind Turbine for Offshore System Development". NREL Technical Report NREL/TP-500-38060.
- Jonkman, J (2010). "Definition of the Floating System for Phase IV of OC3," NREL Technical Report NREL/TP-500-47535.
- Martin, H (2011). *Development of a Scale Model Wind Turbine for Testing of Offshore Floating Wind Turbine Systems*, M.S. Thesis, University of Maine.
- Moon III, WL, Nordstrom, CJ (2010). "Tension leg platform turbine: A unique integration of mature technologies," *Proceedings of the 16th Offshore Symposium, Houston, Texas Section of the Society of Naval Architects and Marine Engineers*.
- Musial, W, Butterfield, S, and Ram, B (2006). "Energy from Offshore Wind," *Offshore Technology Conference*.